

Fe-S cluster binding mechanism of pigeon's ISCA1 clarified by SEC-SAXS

Shigeki ARAI^{1*}, Rumi SHIMIZU¹, Motoyasu ADACHI¹, Mitsuhiro HIRAI²

¹National Institutes for Quantum and Radiological Science and Technology,

2-4 Shirakata, Tokai, Ibaraki 319-1106, Japan

²Graduate School of Science and Technology, Gunma University, 4-2 Aramaki, Maebashi, Gunma 371-8510, Japan

1 Introduction

The iron-sulfur cluster assembly 1 homolog cIISCA1 of *Columba livia* (pigeon) interacts with a quantum biosensor protein cCRY4 [1]. The cCRY4/cIISCA1 complex tends to orientate along the weak external magnetic-field lines (0.4–10G) under blue light, suggesting that cIISCA1 might assist the function of cCRY4. Previously, we clarified that cIISCA1 forms two types of protomers (the globular Type-A and the rod-like Type-B), and the Type-A protomer self-associates to form a columnar oligomer [2]. Moreover, it was expected that the Fe-S cluster binding to cIISCA1 might improve the magnetic property of cIISCA1. In order to elucidate the Fe-S cluster binding mechanism of cIISCA1, we conducted the small angle X-ray scattering analysis coupled with size exclusion chromatography analysis (SEC-SAXS) and UV/Vis spectroscopy.

2 Experiment

SEC-SAXS data were collected with the ACQUITY UPLC H-Class (Waters, Massachusetts, USA), a Superose 6 Increase 10/300 μ l column and a temperature-controlled flowthrough cell (20 °C) that allows UV-vis measurements directly on the SAXS exposure volume. The wavelength used was equal to 1.5 Å. The sample-to-detector distance was 2 m. In the SEC-SAXS measurement, 0.5 ml of 6.9 mg ml⁻¹ cIISCA1 in 20 mM Tris-HCl buffer at pH 8 including 0.15 M NaCl and 10 μ M 3-Mercapto-1-propanol was loaded on the column. The flow rate was set to 0.4 ml min⁻¹ and decreased to 0.05 ml min⁻¹ when the protein eluted from the column to ensure long enough exposure times and accordingly better counting statistics in the obtained data. The SEC-SAXS images corresponding to 20 s of exposure were collected during the elution. Buffer scattering was subtracted from scattering curves of each fraction to yield the sample scattering curve using the program *SAngher* ver. 2.1.33. The averaged gyration radius R_g of eluted components in each fraction was evaluated from the scattering curves at the fraction frame No. 270–330 with the Guinier analysis using the program *Serial Analyzer* ver. 1.3.0.

Moreover, according to the procedure described in [2], the volume fractions of the cIISCA1 components (the Type-A protomer model, the Type-B protomer model, and the oligomer models constructed from those protomers) in each fraction were evaluated by the program *Oligomer* [3].

3 Results and Discussion

The SEC-SAXS elution profile derived from the forward scattering $I(0)$ and UV absorbance at A_{280} of cIISCA1 showed a broad peak at elution No. 240–340 (Fig. 1A). The R_g s evaluated from $I(q)$ s of the elution No. 270–330 with the Guinier analysis decreased from 21.3 to 17.6 Å with the elution progress.

For the oligomer analysis, the theoretical scattering curves ($I_m(q)$ s) calculated from the model structures showed good fitness for the experimental $I(q)$ s at the elution No. 270–330 (Fig. 1B). Fig. 1C shows the volume fractions and shapes of the eluted components estimated by the oligomer analysis. The Type-A monomer was 44.2%–73.2% at the elution No. 270–330. The Type-A dimer was 4.1%–22.0% at the elution No. 270–284, 2.8% at the elution No. 296–300, and 2.0%–7.2% at the elution No. 322–330 (Fig. 1C). The Type-A tetramer or larger oligomers were 1.6%–15.4% at the elution No. 270–302. The Type-B monomer was 6.0% at the elution No. 270 and 2.8%–52.8% at the elution No. 286–330. The Type-B dimer was 5.0%–13.1% at the elution No. 270–274 and 1.5%–22.5% at the elution No. 278–324. The Type-A/Type-B complex and the Type-B oligomer larger than dimer were not detected in all elution ranges.

The UV/Vis absorption spectra of cIISCA1 were also measured simultaneously with the SEC-SAXS measurement (Fig. 2). The absorption peaks at 330 and 420 nm reflecting the Fe–S cluster's existence [1] were obviously larger at the elution No. 270–290 than at the elution No. 295–330. Taken together with the result of the oligomer analysis (Fig. 1C), the UV/Vis absorption spectra indicate that the cIISCA1 oligomers consisting of the Type-A protomer can bind Fe–S clusters and that the Type-A monomer, the Type-B monomer, and the Type-B dimer cannot bind Fe–S clusters. Therefore, the affinity of cIISCA1 to the Fe–S cluster depends on the oligomeric state and the protomer structure of cIISCA1.

A previous study indicated that the interaction between cCRY4 and cIISCA1 is nearly abolished when the Fe–S cluster binding ability of cIISCA1 is lost by the C60A/C124A/C126A mutation [1]. Since the release of Fe–S clusters occurs cooperatively with the conformational change of cIISCA1 from the Type-A protomer to the Type-B protomer (Fig. 1C and 2), it can be considered that the cCRY4/cIISCA1 interaction also needs the Fe–S cluster bound form of cIISCA1, namely, the Type-A protomer.

The 2Fe-2S cluster or 4Fe-4S cluster binding site on protein molecules is formed by four side chains of Cys residues [4]. Since one cIISCA1 molecule has only three Cys, the Fe-S cluster binding site formation on cIISCA1 needs the assembly of more than two Type-A protomers. Therefore, the self-association of Type-A protomers to generate a columnar oligomer would make it possible to build Fe-S cluster binding sites between cIISCA1 molecules. Periodic and regular binding of Fe-S clusters along the long axis of the columnar oligomer may improve the magnetic susceptibility and the magnetic anisotropy of the cIISCA1 oligomer and the cCRY4/cIISCA1 complex.

Acknowledgement

This work was supported by JSPS KAKENHI Grant Number JP18K06174.

References

- [1] Qin S, *et al.*, *Nat Mater.* (2016) 15, 217
- [2] Arai S, *et al.*, *Photon Factory Activity Report 2020 #38* (2021)
- [3] Konarev PV, *et al.*, *J. Appl. Cryst.* 36 (2003) 1277
- [4] Beinert H, *et al.*, *Science.* 277 (1997) 653

* arai.shigeaki@qst.go.jp

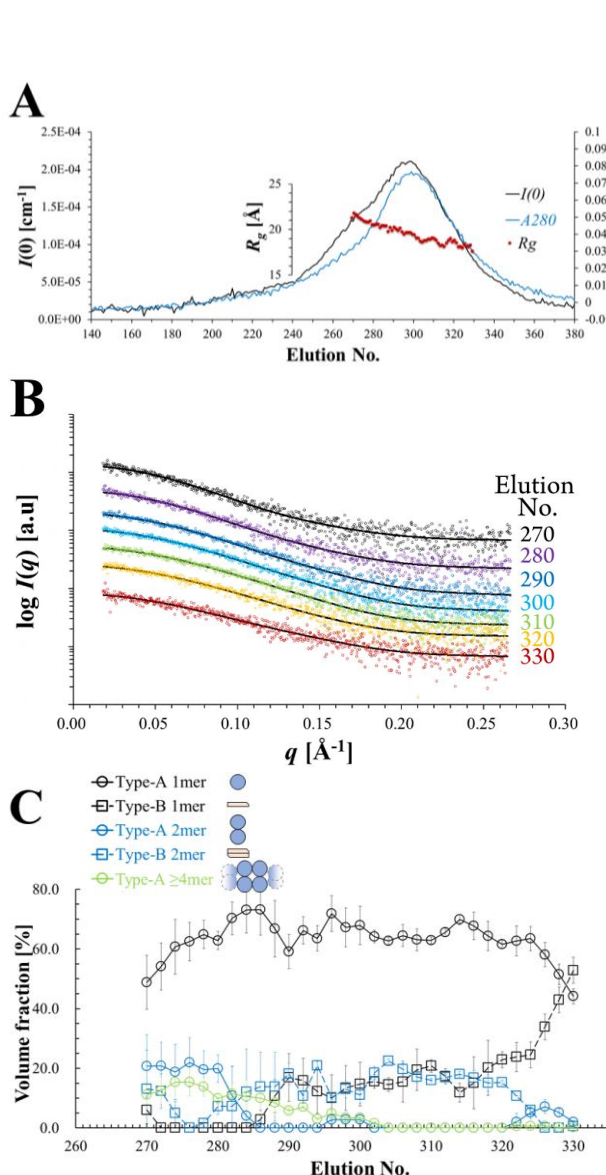


Fig. 1 SEC-SAXS data and oligomer analysis of cIISCA1. (A) SEC-SAXS elution profile of cIISCA1 (line). Dots represent R_g evaluated by the Guinier analysis. (B) The experimental $I(q)$ s at the elution No. 270–330 (dots) and the theoretical $I_m(q)$ s calculated by the oligomer analysis (lines). (C) The volume fractions of the components at the elution No. 270–330.

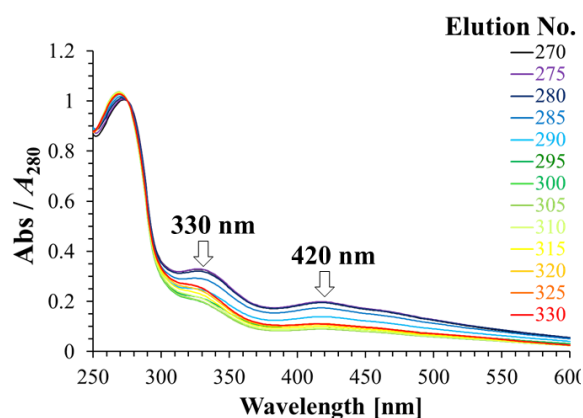


Fig. 2 The UV-vis absorption spectra of cIISCA1 during the elution of SEC corresponding to the elution No. 270–330 of SEC-SAXS. These spectra were normalized by the absorption value at 280 nm.